35th Annual International Conference of the IEEE EMBS
Osaka, Japan, 3 - 7 July, 2013

Distinction between added-energy and phase-resetting mechanisms in non-invasively detected somatosensory evoked responses

T. Fedele. H.-J. Scheer , M. Burghoff , G. Waterstraat, VV Nikulin, G. Curio

Abstract— **Non-invasively recorded averaged event-related potentials (ERP) represent a convenient opportunity to investigate human brain perceptive and cognitive processes. Nevertheless, generative ERP mechanisms are still debated. Two previous approaches have been contested in the past: the added-energy model in which the response raises independently from the ongoing background activity, and the phase-reset model, based on stimulus-driven synchronization of oscillatory ongoing activity. Many criteria for the distinction of these two models have been proposed, but there is no definitive methodology to disentangle them, owing also to the limited information at the single trial level. Here, we propose a new approach combining low-noise EEG technology and multivariate decomposition techniques. We present theoretical analyses based on simulated data and identify in high-frequency somatosensory evoked responses an optimal target for the distinction between the two mechanisms.**

I. Introduction

Event-related potentials/fields are neurophysiological responses detectable non-invasively with EEG/MEG. These evoked responses (ERs) are generated contingent upon a sensory, motor or cognitive event that triggers one or more brain areas to respond, producing an electromagnetic signature detectable at the scalp. This relation between stimulus and ERs allows the investigation of underlying sensorimotor or cognitive processes through the analysis of temporal, spectral and spatial ER features. Nevertheless, even if the brain structure generating the scalp potential can be localised, it remains to be clarified how the stimulus or event is processed locally. Three basic generic models of ER generation have been proposed so far: added-energy, phase-reset, and baseline-shift. In the added-energy model, the stimulus elicits an ER linearly superimposed on the background ongoing activity [1-3]. In the phase-reset model, the stimulus synchronizes the phase of ongoing oscillations [4,5]. In the baseline-shift model, ERs are produced through the amplitude modulation of ongoing oscillations, which do not have zero mean [6]. All three models imply that the ER is phase-locked to the stimulus, and can be distinguished from the background through averaging across many trials. Since the averaged response is not informative about the underlying generating mechanisms, the interest has been in establishing criteria elucidating the underlying neural process [7]. Indicators based on phase and power analysis of pre- and poststimulus temporal intervals can not uniquely discern among different scenarios, mainly because of the low Signal-to-Noise Ratio (SNR) at the level of single trials [8]. Here, we focus on the analysis of the first two mechanisms based on high-frequency somatosensory evoked potentials (hf-SEP) elicited by electrical median nerve stimulation and detected non-invasively with a low-noise custom-made amplifier [9]. Hf-SEP show an extremely stable phase-locking to the stimulus, as outlined in invasive studies [10-11]. In addition, it includes peculiar characteristics in terms of low SNR and neurophysiological significance, as it represents non-invasively detected spike-like brain activity [12]. The present analysis is based on the comparison between two multivariate techiques, Common Spatial Pattern (CSP) and Canonical Correlation Analysis (CCA), as they emphasize different signal properties related to the added-energy and phase-reset generative model. We support the theoretical insight with simulated data, and test our idea on real data, showing consistency with other approaches [13].

II. Methods

A. Simulation

We simulated EEG recordings for 29 channels, computed as the forward projection of N = 500 dipoles. We computed two sets of simulations, one for the added-energy and one for the phase-reset model. Each single trial was considered to have 100 ms duration, sampled at 5 kHz, with 50 ms prestimulus, 50 ms poststimulus. For the generation of noise we used N-1 uncorrelated dipoles mimicking 1/f type of noise, filtered in the frequency range of interest (400-800 Hz). The dipoles have random spatial location and orientation with respect to the scalp. Importantly, this type of noise produces spatial correlations in sensor space. The signal of interest was a pure sinusoidal 600 Hz oscillation, raising with zero phase at the stimulus onset, lasting 50 ms and ranging between -1 and 1. The prestimulus interval was set to zero amplitude in the case of added-energy model, and at a random phase in case of phase-reset model.
The forward model can be written as

$$X = M \times S$$

where X, shaped $(t \times k)$ is the signal detected on the scalp, with t samples and k channels; M, shaped $(k \times N)$ is the

*Supported by Bernstein Focus Neurotechnology-Berlin (B1) and DFG (SFB 618-B4).

T. Fedele, G. Waterstraat, V.V. Nikulin, Gabriel Curio are at Neurophysics Group, Department of Neurology, Campus Benjamin Franklin, Charite – University Medicine Berlin, Hindenburgdamm 30, 12200 Berlin, Germany

M. Burghoff and H.-J.Scheer are at Physikalisch-Technische Bundesanstalt / Institut Berlin, Abbestr. 2-12, 10587 Berlin, Germany.

forward-model lead field matrix, with each column expressing a specific spatial pattern: the first relative to the source pattern, and the others to the noise contribution. All lead field matrix columns were normalized to unitary standard deviation. *S*, shaped (*t* x *N*) is the signal in the N-dimensional source space, with the first source fixed for all trials, and all the others left to vary randomly, in order to resemble an ongoing background activity.
Parameters of the simulation were: i) the SNR calculated at the scalp level as the ratio between the root mean square (rms) of the source projection and the mean of the rms of the N-1 random dipoles projections. The SNR was tuned to vary between 0.01 and 1; ii) the number of trials, ranging between a minimum of 10 and a maximum of 2000. For each iteration the SNR and the number of trials was kept constant. The simulation results are computed as the mean values of 20 iterations, for each combination of SNR and number of trials.

B. Recordings

SEP measurements were performed in three healthy subjects, inside an electrically and magnetically shielded room (Vakuumschmelze AK3b). Sintered Ag/AgCl ring electrodes were placed using a fabric cap with holders at positions according to the 10/20 system. 29 EEG electrodes were distributed over the scalp. The reference was placed on the nasion, and ground on left cheek. The impedances at all electrode–skin interfaces were carefully prepared using standard abrasive paste until for all electrodes values at or below 1 kΩ were achieved; impedance stability was checked and confirmed repeatedly during all measurements.
During the recordings the subject was comfortably resting on a bed in a relaxed supine position. A constant-current square wave electrical stimulus of 200 μs width, 5–8 mA (1.5 times motor threshold) and 0.99 Hz repetition rate was applied transcutaneously to the median nerve at the left wrist. Data were acquired using a bandwidth of 0.16–2000 Hz (total gain 10000, ADC rate 5 kHz, resolution 20 bits). We utilised a low-noise custom-made amplifier, with a white noise level of 4.8 nV/√Hz [9].
Stimulus artifacts were removed in single-trials in each channel by cubic interpolation from -5 to +5 ms around the stimulus onset. Trials exceeding three times the average standard deviation in the frequency range 200–2000 Hz were rejected. In this analysis 2000 trials were considered. The SNR at the scalp was calculated as the ratio between the Linear Spectral Density estimation [μV/√Hz] of the averaged signal and the broadband artifact-free recorded data at the maximum frequency peak of the sigma-band (450-750 Hz).

C. Data Analysis

We compare in the two set of simulations and in the real hf-EEG data the performance of two multivariate analysis techniques: CSP and CCA.
CSP computes the simultaneous diagonalization of two covariance matrices. In our case we divide the data in two parts, extracting and concatenating in the first one the samples in the pre-stimulus interval of all trials, and in the second all samples of the post-stimulus interval. We pre-compute the covariance matrices C_{pre} and C_{post} and used them in the algorithm as follows:

$$\max_{w} \frac{w^T S_d w}{w^T S_d w} \tag{1}$$

with

$$S_d = (C_{post} - C_{pre})$$
$$S_c = (C_{post} + C_{pre})$$

obtaining $\boldsymbol{w}$, the spatial filter maximizing the ratio of variances between the two classes, in our case the ratio of power between the ER and the baseline at the single trial level. In practice, $\boldsymbol{w}$ is computed by solving a generalized eigenvalue problem and ordered according to the corresponding eigenvalues which were normalized to represent the ratio of variances between the two classes. Subsequently we chose the spatial filter corresponding to the highest eigenvalue for further analysis.
CCA computes the canonical correlation for two data sets, X and Y, finding two sets of basis vectors $\boldsymbol{w_x}$, $\boldsymbol{w_y}$, such that the correlation $\boldsymbol{\rho}$ between the projections of the variables onto these basis vectors are mutually maximized.

$$\max_{w_x, w_y} \quad \rho = \frac{E[xy]}{\sqrt{E[x^2]E[y^2]}} \tag{2}$$
$$= \frac{E[w_x^T x^T y w_y^T]}{\sqrt{E[w_x^T x^T x w_x]E[w_y^T y^T y w_y]}}$$
$$= \frac{w_x^T C_{xy} w_y^T}{\sqrt{w_x^T C_{xx} w_x w_y^T C_{yy} w_y}}$$

In our case the two classes are built by splitting the data set in two subsets, e.g., odd and even trials, and assigning the poststimulus interval to the classes *x* and *y* respectively. It should be noted that $\boldsymbol{w_x}$ and $\boldsymbol{w_y}$ are practically equal if the classes x and y are drawn from the same sample. Thus we chose the spatial projection $\boldsymbol{w_x}$ corresponding to the highest correlation between odd and even trials for further analysis.
The idea to use the result of these two methods as a measure for differentiating between added-energy and phase-reset is that the first relies on the ratio of variances between pre- and poststimulus interval at the single-trial level, and therefore should perform better in the case of added-energy, while the second does not depend on the generative mechanism, solely

finding a spatial pattern that maximizes the trial-to-trial synchronization.

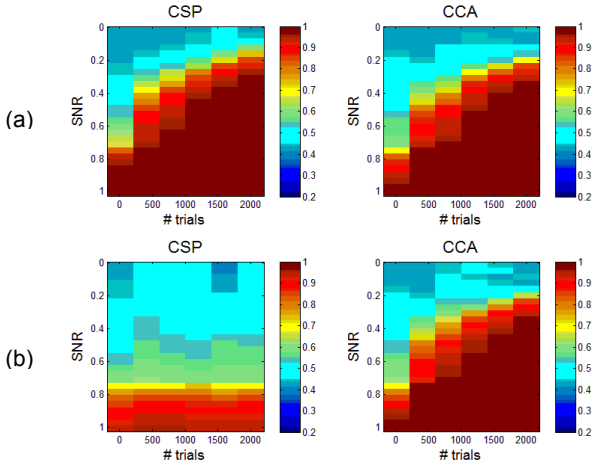

Figure 1. Simulation results in terms of spatial correlation $\rho_{spatial} = < P_{est}, P_{source} >$ between the coefficients of the estimated pattern P_{est}, and the orginal pattern P_{source}, for the two algorithms, CSP and CCA, for the considered span of SNR and number of trials. (a) Added-energy model; (b) Phase-reset model.

For the simulated data, the performance of CCA and CSP for the two generative models is presented for
all combinations of SNR and number of trials in terms of a spatial correlation $\rho_{spatial}$ between the coefficients of the estimated pattern P_{est}, and the original pattern P_{source},

$$\rho_{spatial} = \left\langle P_{est}, P_{source} \right\rangle \qquad (3)$$

For the real data, EEG is pre-filtered in the sigma-band (450-750 Hz), then CSP and CCA are applied and the extracted patterns are compared. Prior to the multivariate analysis, temporal windows of interest are defined. For the pre-stimulus window we set the interval ranging from -40 to -10 relative to the stimulus onset, while the signal window is set to 20 to 30 ms post-stimulus, as in this interval the cortical contribution to hf-SEP is maximal.

III. RESULTS

Our generalized biophysical representation of the two mechanisms provided synthetic scalp data, which was utilized for multivariate analysis. Fig. 1 displays the performance the two methods, Common Spatial Pattern (CSP) and Canonical Correlation Analysis (CCA) on the outcome of the simulation. The spatial correlations $\rho_{spatial}$ between estimated pattern and known source pattern are color-coded for different number of trials and SNR (x and y axis of each subplot). The first row (a) describes the algorithms' performance in the added-energy model. The second row (b) refers to the phase-reset model. Comparable pre- and post-stimulus variance at the source level (b) is found to entail a lower reliability in CSP if SNR<0.8

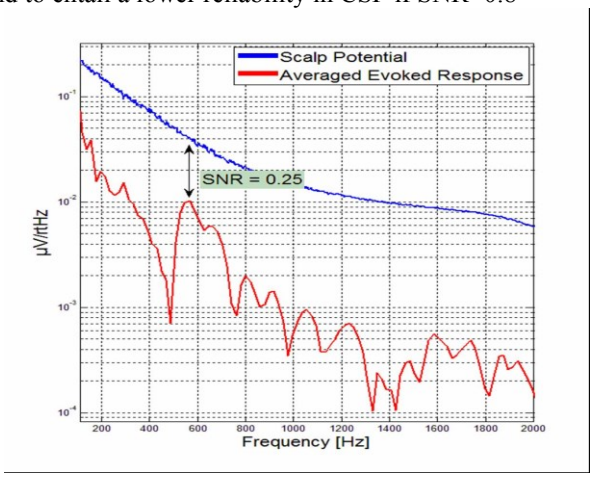

Figure 2. The SNR at the scalp is expressed as ratio between the Linear Spectral Density estimation [μV/√Hz] of the averaged signal (red) and the broadband artifact-free recorded raw data (blue) at the maximum frequency peak of the sigma-band (450-750 Hz).

whereas CCA detects correctly the source pattern, independently from the generative model. As expected, the different theoretical framework supporting the two methods allows us to identify a sensitivity threshold, in terms of number of trials and SNR.
Analysing the spectral representation of the experimental hf-SEP, we estimated a SNR = 0.25, as shown in Fig. 2 for one representative subject; results for the other two subjects are reported in Tab.1.
According to the simulation results, with an SNR = 0.25 CCA should outperform CSP for a phase reset condition, while both algorithms should be equivalent for the added-energy condition. Estimated patterns of real hf-SEP data are presented in Fig. 3. The high level of similarity, with a scalar product approaching unity, argues for an added-energy condition. A further physiological validation is given by comparison to published studies which already described similar spatiotemporal features of hf-SEP [13-15].

Table 1.

SUB JECT	SNR	$< P_{CSP}, P_{CCA} >$
SUBJECT 1	0.25	0.99
SUBJECT 2	0.22	0.91
SUBJECT 3	0.2	0.84

Table 1. For each subject the estimated SNR and spatial correlation coefficient between CSP and CCA patterns are reported.

IV. CONCLUSION

The distinction between added-energy and phase-reset mechanisms from non-invasive data represents a critical

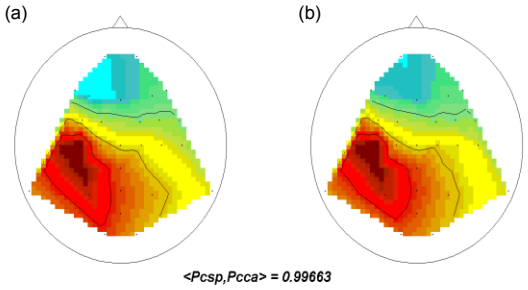

Figure 3. Patterns estimated from hf-SEP data with (a) CSP and (b) CCA. The similarity is expressed in terms of the scalar product between pattern coefficients.

challenge in human neuroscience. SNR is of paramount importance in order to provide sufficient information already
at single-trial level. Here, we present procedural progress enabled by combining low-noise EEG technology with two multivariate analysis techniques. Taken together, a higher sensitivity at the level of scalp data allows to infer on synchronous neural responses which otherwise would be possible only using invasive recordings.

REFERENCES

[1] Mäkinen V, Tiitinen H, May P. Auditory event-related responses are generated independently of ongoing brain activity. Neuroimage 24: 961–968, 2005.

[2] Mazaheri A, Jensen O. Posterior alpha activity is not phase-reset by visual stimuli. Proc Natl Acad Sci USA 103: 2948–2952, 2006.

[3] Shah AS, Bressler SL, Knuth KH, Ding M, Mehta AD, Ulbert I, Schroeder CE. Neural dynamics and the fundamental mechanisms of event-related brain potentials. Cereb Cortex 14: 476–483, 2004.

[4] Fell J, Dietl T, Grunwald T, Kurthen M, Klaver P, Trautner P, Challer C, Elger CE, Fernández G. Neural bases of cognitive ERPs: more than phase reset. J Cogn Neurosci 16: 1595–1604, 2004.

[5] Makeig S, Westerfield M, Jung T, Enghoff S, Townsend J, Courchesne E, Sejnowski T. Dynamic brain sources of visual evoked responses. Science 295: 690–694, 2002.

[6] Nikulin VV, Linkenkaer-Hansen K, Nolte G, Lemm S, Müller KR, Ilmoniemi RJ, Curio G. A novel mechanism for evoked responses in the human brain. Eur J Neurosci 25: 3146–3154, 2007

[7] Sauseng P, Klimesch W, Gruber WR, Hanslmayr S, Freunberger R, Doppelmayr M. Are event-related potential components generated by phase resetting of brain oscillations? A critical discussion. Neuroscience 146: 1435–1444, 2007.

[8] Telenczuk B, Nikulin VV, Curio G. Role of neuronal synchrony in the generation of evoked EEG/MEG responses. J Neurophysiol 2010;104:3557–67.

[9] Scheer HJ, Sander T, Trahms L. The influence of amplifier, interface and biological 784 noise on signal quality in high-resolution EEG recordings. Physiol Meas 27: 109-117, 785 2006.

[10] Baker, S.N., Curio, G., and Lemon, R.N. 2003. EEG oscillations at 600 Hz are macroscopic markers for cortical spike bursts. J. Physiol. 550:529–534.

[11] Hanajima R, Chen R, Ashby P, Lozano AM, Hutchison WD, Davis KD, Dostrovsky 680 JO. Very fast oscillations evoked by median nerve stimulation in the human thalamus 681 and subthalamic nucleus. J Neurophysiol 92: 3171-3182, 2004.

[12] Ozaki I, Hashimoto I. Exploring the physiology and function of high-frequency oscillations (HFOs) from the somatosensory cortex. Clin Neurophysiol 2011;122:1908–23.

[13] Waterstraat G, Telenczuk B, Burghoff M, Fedele T, Scheer HJ, Curio G, Are high-frequency (600 Hz) oscillations in human somatosensory evoked potentials due to phase-resetting phenomena?Clin Neurophysiol. 2012 Oct;123(10):2064-73

[14] Curio G, Mackert B-M, Burghoff M, Koetitz R, Abraham-Fuchs K, Härer W. Localization of evoked neuromagnetic 600 Hz activity in the cerebral somatosensory system. Electroencephalogr Clin Neurophysiol 1994;91:483–7.

[15] Gobbele, R., Buchner, H., and Curio, G. 1998. High-frequency (600 Hz) SEP activities originating in the subcortical and cortical human somatosensory system. Electroencephalogr. Clin. Neurophysiol. 108:182–189.